Available online at www.sciencedirect.com

ScienceDirect

Mendeleev Commun., 2019, **29**, 312–314

Mendeleev Communications

Electrocatalytic properties of a Pd^0(Pb) composite synthesized by galvanic displacement: activity towards formic acid oxidation

Boris I. Podlovchenko,* Yurii M. Maksimov and Dmitry O. Shkil

Department of Chemistry, M. V. Lomonosov Moscow State University, 119991 Moscow, Russian Federation. Fax: +7 495 939 0171; e-mail: podlov@elch.chem.msu.ru

DOI: 10.1016/j.mencom.2019.05.024

Galvanic displacement of electrodeposited lead by palladium fails to produce Pd shells. The anomalous ratio between formic acid electrooxidation reaction (FAOR) rates on Pd^0(Pb) observed in $HClO_4$ and H_2SO_4 solutions is associated with the reduction of ClO_4^- anions to chloride ones which inhibit the FAOR.

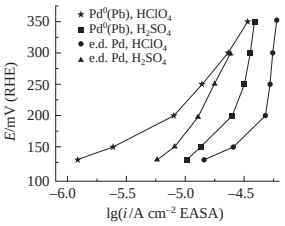

Formic acid is a promising fuel for compact power sources.[1] As earlier, the quest for catalysts of formic acid electrooxidation reaction (FAOR) is preferentially concentrated on palladium-based composites, although recent prices for Pd exceed those for Pt. Interest in Pd is determined by its higher activity in FAOR, as compared with that of other platinum group metals.[1–3] The activity of palladium in FAOR can be considerably increased by mixing it with much cheaper metals M (Ag, Sn, Cu, Co, *etc.*).[4–10] Among the Pd–M systems, mixed Pd–Pb catalysts are least studied.[11] Previously, we found[12,13] that the galvanic displacement (GD) of electrodeposited (e.d.) Pb by platinum ($PtCl_4^{2-}$ as a displacing agent) produced Pt^0(Pb) composites, which exhibited high FAOR activity. It was of interest to carry out an analogous study in the e.d. Pb–Pd^{2+} system. We used gold as a substrate for deposition because it provides a better reproducibility of results, as compared with glassy carbon.

Lead was deposited on a plate (1 cm^2) of polycrystalline gold at E_{dep} = –200 mV from a 0.01 M $PbCO_3$ + 0.1 M $HClO_4$ solution in an amount of 280 ± 15 μg (deposit thickness, ~0.25 μm). The electrochemical cell, GD procedure, reagents (other than $PdCl_2$ from Aldrich), instruments, and methods used for the physicochemical characterization of samples were described earlier[12–14] (see also Online Supplementary Materials). The fundamental difference of measurements performed in this study is that the GD was carried out in a 10^{-3} M $PdCl_2$ + 10^{-2} M $Pb(ClO_4)_2$ + 0.1 M $HClO_4$ solution in place of a solution containing $PtCl_4^{2-}$. The working electrode potentials were measured with respect to a reversible hydrogen electrode (RHE) in the same solution. The activity of the Pd^0(Pb) composite was tested based on stationary FAOR currents observed in 0.5 M HCOOH + 0.1 M $HClO_4$ or 0.5 M HCOOH + + 0.5 M H_2SO_4 solutions (a stationarity criterion corresponded to $dI/d\tau < 1\% I$ min^{-1}) at 20 ± 1 °C.

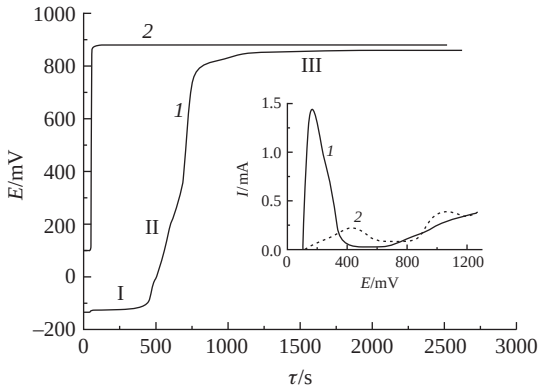

Figure 1 Transients of open-circuit potential upon the introduction of (*1*) e.d. Pb into contact with 0.01 M $Pb(ClO_4)_2$ + 0.005 M $PdCl_2$ and (*2*) e.d. Pd with 0.005 M $PdCl_2$. Supporting electrolyte, 0.1 M $HClO_4$. For description of segments I–III, see the text. Insert: anodic potentiodynamic curves of e.d. Pd in (*1*) 0.1 M $HClO_4$ and (*2*) 0.01 M $Pb(ClO_4)_2$ + 0.1 M $HClO_4$.

The transient of open-circuit potential observed upon the contact of e.d. Pb with the 0.1 M $HClO_4$ + 0.01 M $Pb(ClO_4)_2$ + 0.005 M $PdCl_2$ solution (Figure 1, curve *1*) had a similar shape as the transient corresponding to the displacement of lead by platinum in a $PtCl_4^{2-}$ solution.[12] In segment I, which resembles a plateau, the potential is determined by the reaction Pb ⇄ Pb^{2+} + 2e. Insofar as the GD process occurs at negative potentials, hydrogen evolution should take place on the formed Pd^0 atoms and/or clusters (Pb + Pd^{2+} → Pd^0 + Pb^{2+}). Electrons for this reaction are also supplied by lead dissolution, which partly proceeds *via* the overall reaction Pb + $2H^+$ → Pb^{2+} + H_2. In segment II, the total charge Q of the formed Pd^0(Pb) composite increased.[13–15] These two regions are well distinguishable: the region of slow potential increase (~–50 to +300 mV) and the region of its fast growth (~300–800 mV). The low potential region corresponds to the absorption [both in β and α phases of Pd(H)] and adsorption of hydrogen by palladium. This considerably increases Q (in the absolute magnitude), which is the reason for the slower potential variation at E < 300 mV as compared with E > 300 mV.

In segment III, the stationary potential is established ($dE/d\tau$ < < 0.1 mV min^{-1}; substitution time, 40–45 min), which is close to the potential reached upon contact of e.d. Pd (E_{dep} = 0.25 V, 300 μg)[14] with a 0.1 M $HClO_4$ + 0.005 M $PdCl_2$ solution (curve *2*). The values of E_{st} fall into the potential region of formation of

Table 1 Bulk and surface composition of Pd^0(Pb).

Analysis method	Pd (at%)	Pb (at%)
ICP-AES	86.4 (92.5 μg)	13.6 (28.5 μg)
EDX	89.2	10.8
XPS	87.7	12.3

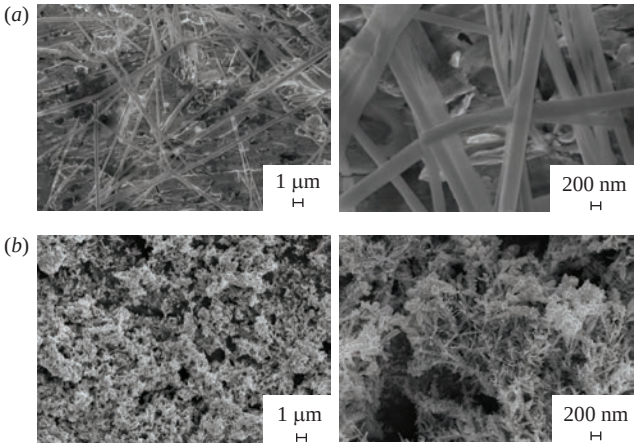

Figure 2 SEM images of (*a*) e.d. Pb and (*b*) Pd^0(Pb).

palladium oxides. The closeness of the E_{st} values for Pd^0(Pb) composites formed here and e.d. Pd (Figure 1) allows us to assume that lead is contained in small amounts in the surface layer of Pd^0(Pb) [by analogy with Pt^0(Pb)[12,13]].

All of the samples were thoroughly washed with a deaerated background solution and then with twice-distilled water before their *ex situ* characterization. According to Figure 2(*a*), the original Pb deposit on polycrystalline Au consists of crystals of various shapes and of long (>10 μm) cylindrical fibers. The latter are preferentially localized in the surface layer. Because of GD, the deposit morphology considerably changes: the deposit loosens and acquires a coral-like structure [Figure 2(*b*)].

According to the results of energy dispersive X-ray (EDX) spectroscopy (Figure S1, Online Supplementary Materials), Pd and Pb in the mixed deposit are distributed sufficiently uniformly over the substrate surface with an average lead content of ~11 at% (Table 1, Pd + Pb = 100%).

A close value (~13.5 at%) was obtained by inductively coupled plasma atomic emission spectroscopy (ICP-AES). All intermetallides formed in the Pd–Pb system have a lead content of no lower than 25 at%;[16] hence, no intermetallides can be formed during the GD of Pb by Pd. A comparison of the mass of original e.d. Pb with the masses of Pd and Pb in the Pd^0(Pb) composite allows us to conclude that ~30% of lead passes to solution *via* the overall reaction $Pb + H^+$.

According to XPS data (Figure S2 and S3, Online Supplementary Materials), in the surface layer of Pd^0(Pb), the components are present in the atomic ratio Pd : Pb = 1 : 0.14; *i.e.*, the Pb content is ~12 at%, which almost coincides with the volume content of lead. Hence, no Pd shell is formed. Probably, the reason for this is the incomplete desorption of Pb adatoms

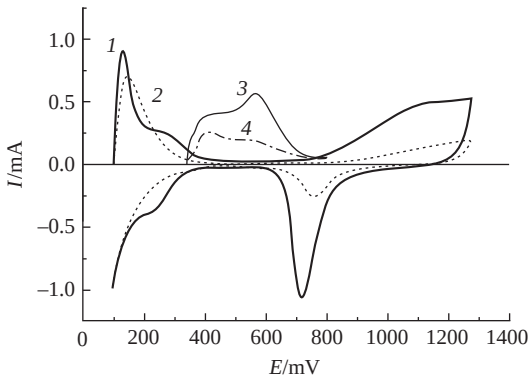

Figure 3 CVA of (*1*) Pd^0(Pb) and (*2*) e.d. Pd; curves of Cu_{ad} electrodesorption from (*3*) Pd^0(Pb) and (*4*) e.d. Pd. Supporting electrolyte, 0.1 M $HClO_4$.

(Pb_{ad}) from Pd particles at $E \leqslant E_{st}$.[12,13] Indeed, a bond between Pb_{ad} and Pd is indirectly confirmed by the strong inhibition of hydrogen sorption in the presence of Pb_{ad}, as follows from a comparison of hydrogen regions (see Figure 1, insert, curves *1* and *2*). For Cu_{ad}, such effect was not observed.[17]

From the XPS data, it was determined that in the surface layer of the composite, palladium was present as Pd^0 and lead as Pb^0 (81 at%) and Pb^{2+} (19 at%). Inside the particles, there was obviously Pb^0. According to X-ray diffraction (XRD) data, the Pd lattice parameter in the composite increased (3.915 Å against a table value of 3.890 Å) to indicate the dissolution of Pb^0 in palladium. Note that Pb^{2+} may appear because of lead oxidation in contact with air before the XPS measurements.

Figure 3 compares an anodic potentiodynamic curve on freshly formed Pd^0(Pb) composite (curve *1*) with an analogous curve on e.d. Pd (curve *2*). The areas under hydrogen regions of two samples are sufficiently close; it is only the energy spectra of removal of sorbed hydrogen that differ. At the same time, the area under the oxygen regions of curve *1* much exceeds an analogous area in curve *2*. The close shapes of *I vs. E* curves for Pd^0(Pb) and e.d. Pd in the potential region under consideration suggest that the effect is mainly caused by difference in the electrochemically active surface areas (EASAs) of two deposits. This is confirmed by the curves of removal of monolayers (ML) of copper adatoms (curves *3* and *4*). The EASA values estimated with respect to Cu_{ad} (420 μC cm^{-2} per Cu ML[17]) were found to be 13.4 cm^2 for Pd^0(Pb) and 4.6 cm^2 for e.d. Pd. Taking into account the difference in the amounts of Pd in two samples (Table 1), the specific EASA values are 14.5 m^2 g^{-1} Pd for Pd^0(Pb) and 2.5 m^2 g^{-1} Pd for e.d. Pd. Thus, the galvanic displacement produced a much more dispersed deposit as compared with the electrodeposition method.

We assume that the electrodesorption of a H_{ads} monolayer consumes the charge Q_{MLH} equal to $0.5Q_{MLCu}$.[17] Then, by subtracting $0.5Q_{MLCu}$ from the charge consumed in the ionization of sorbed hydrogen (see Figure 3, curves *1*, *3* and *2*, *4*), we can roughly estimate the amount of dissolved hydrogen in the Pd(H) α-phase for two samples. Calculations have shown that hydrogen much better dissolves in the α-phase of Pd^0(Pb) (~1.4 mmol H_2 per cm^3 of Pd), as compared with e.d. Pd (~0.45 mmol cm^{-3}). This points out the higher defectiveness of the Pd structure in Pd^0(Pb) as compared with e.d. Pd.[17]

The specific stationary currents of FAOR in a sulfuric acid solution at E < 400 mV are of the highest interest for direct formic acid fuel cell (DFAFC). On Pd^0(Pb), they turned out to be approximately double the currents on e.d. Pd (Figure 4, curves *2* and *4*). Thus, we observed a relatively weak promotion effect of the presence of lead in the composite on the electrocatalytic activity of Pd in FAOR. The effect was much weaker than that in the case of platinum activation by lead additions: for Pt^0(Pb) composites, an increase in FAOR activity was higher by one or two orders of magnitude as compared with e.d. Pt.[12,13] Numerous factors capable of promoting the effect of lead additions were discussed previously.[12] Their diversity makes it difficult to explain a considerable difference in the effects of Pb on the activity of Pd and Pt.

Quite unexpected were the results of a comparison between FAOR activities of Pd^0(Pb) and e.d. Pd samples in the 0.1 M $HClO_4$ solution (see Figure 4, curves *1* and *3*). The currents on Pd^0(Pb) were much lower than those on e.d. Pd, and this is inconsistent with the results obtained in sulfuric acid solution. Moreover, in a potential interval of 150–300 mV, the FAOR currents on Pd^0(Pb) in $HClO_4$ solution (curve *1*) were substantially lower than analogous currents in H_2SO_4 solution (curve *2*). Taking into account the weaker adsorption of ClO_4^- anions as compared with SO_4^{2-} (HSO_4^-) anions, we expected the opposite

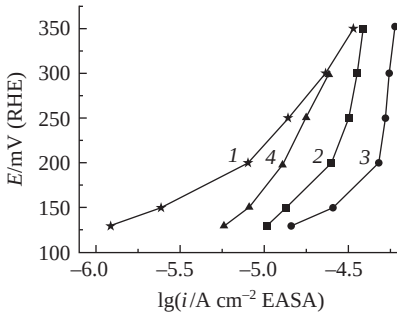

Figure 4 Stationary polarization curves of FAOR on (*1*,*2*) Pd^0(Pb) and (*3*,*4*) e.d. Pd in (*1*,*3*) 0.5 M HCOOH + 0.1 M $HClO_4$ and (*2*,*4*) 0.5 M HCOOH + + 0.5 M H_2SO_4 solutions.

dependence of the FAOR current on the nature of anion. These remarkable results allowed us to assume that the FAOR on Pt^0(Pb) is accompanied by the simultaneous reduction of ClO_4^- anions to Cl^- anions and the latter specifically adsorb thus inhibiting the FAOR. The inhibiting effect of chloride anions on chemisorption and electroreduction of simple organic substances is well known.[18,19]

On e.d. Pd, the FAOR currents in $HClO_4$ solution (curve *3*) exceed analogous currents in H_2SO_4 solution (curve *4*), *i.e.*, no inhibition of FAOR by Cl^- anions is observed or it is insignificant. Hence, the incorporation of Pb into Pd deposit catalyzes the reduction of ClO_4^- anions. Such an effect of lead can be associated with its oxophilicity. According to published data,[20] the electroreduction of ClO_4^- anions on oxophilic metals proceeds at a considerable rate.

To check the above explanation of anomalously low FAOR currents on Pd^0(Pb) in perchlorate solutions, we carried out the following experiment: after the polarization of Pd^0(Pb) in a 0.5 M HCOOH + 0.1 M $HClO_4$ solution for 4 h (a cell with separated anodic and cathodic compartments, E = 300 mV), the solution was tested for the appearance of chloride ions. The addition of $AgNO_3$ to the solution after FAOR led to pronounced turbidity due to the formation of AgCl (in the original solution, this effect was absent). After an analogous experiment with e.d. Pd, the appearance of Cl^- in the solution was not detected. In agreement with published data,[20] this result shows that the polarization measurements in $HClO_4$ solutions should be interpreted with caution bearing in mind the possible reduction of ClO_4^- anions.

This work was supported in part by the M. V. Lomonosov Moscow State University Programme of Development. We are grateful to E. E. Levin and K. I. Maslakov for their help in EDX and XPS measurements.

Online Supplementary Materials

Supplementary data associated with this article can be found in the online version at doi: 10.1016/j.mencom.2017.05.024.

References

1 N. V. Rees and R. G. Compton, *J. Solid State Electrochem.*, 2011, **15**, 2095.
2 A. Capon and R. Parsons, *J. Electroanal. Chem.*, 1973, **44**, 239.
3 K. Jiang, H.-X. Zhang, S. Zou and W.-B. Cai, *Phys. Chem. Chem. Phys.*, 2014, **16**, 20360.
4 R. S. Batalov, V. V. Kuznetsov, B. I. Podlovchenko and V. A. Zaytsev, *Mendeleev Commun.*, 2017, **27**, 583.
5 Z. Zhang, J. Ge, L. Ma, J. Liao, T. Lu and W. Xing, *Fuel Cells*, 2009, **9**, 114.
6 D. Morales-Acosta, J. Ledesma-Garcia, L. A. Godinez, H. G. Rodriguez, L. Álvarez-Contreras and L. G. Arriaga, *J. Power Sources*, 2010, **195**, 461.
7 Yu. M. Maksimov, B. I. Podlovchenko, E. M. Gallyamov, S. A. Dagesyan, V. V. Sen and S. A. Evlashin, *Mendeleev Commun.*, 2017, **27**, 382.
8 L. Dai and S. Zou, *J. Power Sources*, 2011, **96**, 9369.
9 S. Hu, L. Scudiero and S. Ha, *Electrochem. Commun.*, 2014, **38**, 107.
10 Q. Zhao, J. Wang, X. Huang, Y. Yao, W. Zhang and L. Shao, *Electrochem. Commun.*, 2016, **69**, 55.
11 R. Li, H. Hao, W.-B. Cai, T. Huang and A.Yu, *Electrochem. Commun.*, 2010, **12**, 901.
12 B. I. Podlovchenko and Yu. M. Maksimov, *J. Electroanal. Chem.*, 2017, **801**, 319.
13 Yu. M. Maksimov, B. I. Podlovchenko, D. S.Volkov, K. I. Maslakov and S. A. Evlashin, *Mendeleev Commun.*, 2019, **29**, 83.
14 B. I. Podlovchenko, Yu. M. Maksimov, K. I. Maslakov, D. S. Volkov and S. A. Evlashin, *J. Electroanal. Chem.*, 2017, **788**, 217.
15 B. I. Podlovchenko, N. A. Epshtein and A. N. Frumkin, *J. Electroanal. Chem.*, 1974, **53**, 95.
16 *ASM Handbook, Vol. 3: Alloy Phase Diagrams*, ASM International, Materials Park, OH, 1992, sect. 2, p. 333.
17 B. I. Podlovchenko, E. A. Kolyadko and S. Lu, *J. Electroanal. Chem.*, 1995, **399**, 21.
18 T. Iwasita, *Electrochim. Acta*, 2002, **47**, 3663.
19 N. Job, M. Chatenet, S. Berthon-Fabry, S. Hermans and F. Maillard, *J. Power Sources*, 2013, **240**, 294.
20 G. G. Lang and G. Horanyi, *J. Electroanal. Chem.*, 2003, **552**, 197.

Received: 18th December 2018; Com. 17/5781